A Heat Transfer Finite Element Model for Wire-Arc-Additive-Manufacturing Process

Y. Ling, J. Ni, Magd Abdel Wahab, J. Antonissen, and J. Vande Voorde

Abstract This paper presents a part of work to develop a suitable numerical tool to define printing strategy for Wire-Arc-Additive-Manufacturing (WAAM) process. Based on previous research work, A three dimensional metallo-thermo-mechanical model on welding process are transplanted through Abaqus CAE and user subroutines for the simulation of WAAM process. A test plate manufactured by WAAM processing is used as the validation of the simulation. In this paper, heat transfer modelling for WAAM process is presented, which includes two key issues, namely a modified Goldak model for heat source and interval layer forced cooling parameters. The modified Goldak model is capable to simulate energy input of filler material correctly. The inter layer idle time and forced cooling flux are very crucial to the geometry, and the quality of the fabricated part by WAAM process. The ambition of this project is to use desired properties as input parameters of the simulation tool and obtain output parameters to define the optimized strategy for WAAM process.

Keywords WAAM · FEM simulation · Strategy · Welding · Additive manufacturing

Y. Ling (✉) · J. Ni · M. Abdel Wahab
Laboratory Soete, Faculty of Engineering and Architecture, Gent University, 9052 Zwijnaarde, Belgium
e-mail: Yong.Ling@UGent.be

J. Antonissen
Guaranteed B.V., 9060 Zelzate, Belgium

J. Vande Voorde
OCAS.N.V, 9060 Zelzate, Belgium

1 Introduction

Additive manufacturing is one of the intelligent manufacturing topics in recent years. Wire-Arc-Additive-Manufacturing (WAAM) is the most efficient process in deposition rate (2–10 kg/h) [1] and one of its big advantages is its capability to make large metal structure parts especially in offshore engineering [2]. Currently, the international state of the art in wire arc additive manufacturing (WAAM) of large scale steel components mainly focuses on making good shape and less defects in the components. Many uncertainties remain in correlations of the final functional properties to the printing material and strategy. The research goal therefore is using the desired properties for the outputs of printing parameters in order to control the quality of the components. The plan envisages to develop both the missing modelling tools as well as the experimental screening capabilities to facilitate a swift industrial uptake of WAAM for safe and cost efficient production of large scale industrial components which bear a safety-critical function [3]. Figure 1 shows the frame diagram of the objectives.

Typically, WAAM process is very similar to automatic gas metal arc welding process(GMAW) [8]. It was called as shape welding(SW), rapid prototype welding(RP), as well as 3D welding. Modelling welding process is related to describe multi physical phenomena mathematically which includes arc burning and high temperature gas flow, heat energy transfer, melting metal drop forming and weld molten pool moving, and so on. Of course it is not possible to model whole complex process. However many research works have been done and some knowledge currently have been adopted to WAAM process. Simulation tool becomes efficient and economical approach to play a key role in making the strategy for WAAM process. The numerical tool to be developed here is a kind of AI (artificial intelligent) operator. Ideally inputting desired phases fractions or mechanical properties of the part to the tool one can obtain the optimized output parameters such as current, voltage, moving speed and filler melting velocity for the printing processing. Rodrigues et al. published the current status and perspectives on WAAM.
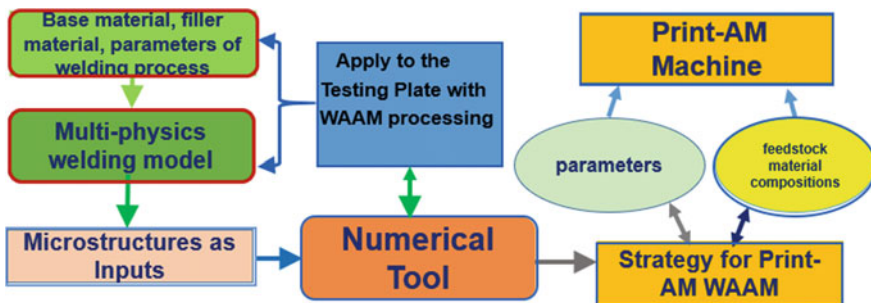

Fig. 1 Frame diagram of the objectives

Many researchers worked on multi-physical modelling on Additive manufacturing and many publications were reported [4–7].

Practically, WAAM is multilayer and multi pass welding process. In this work the 3D test plate was simulated by using Abaqus CAE 2019 and user subroutines with the thermo-metello-mechanical model developed by Ni for welding process simulation [9]. To examine the effects of models on WAAM process heat source Goldak model and modified Goldak heat source model are applied. Heat transfer simulations with real printing parameters were devoted, which include arc current, voltage, moving velocity and wire feeding speed. To simulate the results of the experiments, algorithms in Abaqus for convection and film sink for interval layer cooling were adopted. Obviously the quality and functionality of the AM component is affected directly by the selected parameters of printing processing. Due to the complexity of WAAM process, it is necessary to define the right strategy to obtain a desired functional component despite of the existence of many challenges.

2 Heat Source Input
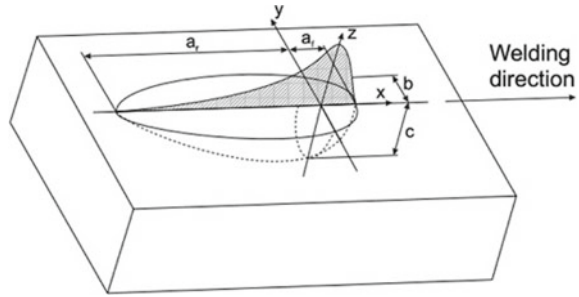
2.1 Heat Source Models

Good Modelling of heat source input is a significant issue, which relates to WAAM parameters directly. As reviewed in the PhD dissertation of Ni, many research works have been done [10]. The first distributed heat source model was proposed by Pavelic [11], in which a Gaussian distribution of heat flux was assumed to be deposited on the surface of the sample. This was appropriate for modelling heat source of low power density. *Krutz* and *Segerlind* [12] proposed a modified form of this model. If the heat source moves at x–z plane and along x direction, the heat flux q_{in} is expressed as [13]:

$$q\mathrm{in} = \frac{3Q_{in}}{\pi c^2} \exp\left(-\frac{3[x + v(t - t_0)]^2}{c^2} - \frac{3z^2}{r_c^2} \right) \tag{1}$$

where r_c is the characteristic radius of the heat flux distribution. t_0 is the time at which the heat source original action point and t is the current time, and v is the moving speed.

Goldak et al. [14] developed a non-axisymmetric three dimensional (3D) heat source model that could simulate complex weld pool. As shown in Fig. 2, the most general form was created by distinguishing ellipsoid semi-axes in front and rear quadrants. This model is known as double ellipsoid model and widely used in the simulation of welding process. Equation (2) is the power density distribution function:

Fig. 2 Goldak double ellipsoid model

$$\dot{q}_v = \frac{6\sqrt{3}\dot{Q}\,f_{f\cdot r}}{a_{f,r}bc\pi\,\sqrt{\pi}}\exp\left(-\frac{3x^2}{a_{f\cdot\gamma}^2} - \frac{3y^2}{b^2} - \frac{3z^2}{c^2}\right) \tag{2}$$

This heat source model defined two different power distribution functions for positive and negative x semi axes. It modeled asymmetric heat power distribution over the molten pool. $a_{f,r}$, b and c are the semi axes of two ellipsoids centered in the origin of the frame of reference, as described in Fig. 2. The parameter a has different values depending on x sign (a_f if positive and a_r if negative) [15]. Usually the values of ellipsoids semi axes are set according to molten pool dimensions [16]. $f_{f,r}$ are the distribution factors, which are f_f the frontward and f_r backward ellipsoids, and the following condition is fulfilled [14]:

$$f_f + f_r = 2 \tag{3}$$

where $\dot{Q}$ is the heat input rate computed as the product of welding current I, welding voltage V and arc efficiency η.

$$\dot{Q} = \eta IV \tag{4}$$

The integrating form of the two power density functions in spatial coordinates gives the total energy rate generated by the heat source as [14].

$$\int\limits_{-\infty}^{+\infty}\int\int \dot{q}_v(x, y, z)dxdydz = 2\dot{Q} \tag{5}$$

In this model, the real power transmitted to workpiece depends upon the relative position between the heat source frame of reference and the base material. If the origin is positioned on the top surface of the substrate the heat input is transmitted to both of the base and filler material. According to Eq. (5) the heat power transmitted is higher than the actual process heat input $\dot{Q}$. It will result in overheat of molten pool temperature. On the other hand, if the origin positioned on the top of filler material

Fig. 3 The modified Goldak model

Welding direction
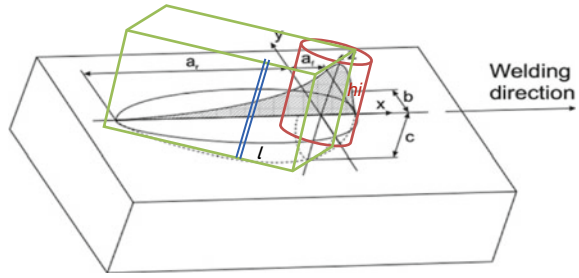
the heat power transmitted would be good but it will result in a poor weld penetration on the base material [16]. Since most of heat is delivered to the filler material.

Montevecchi et al. proposed modified Goldak model [17]. This model divides heat source power into two parts. The power for melting filler metal is about 50% of total arc power [18]. The main improvement is capable to take the parameter of filler melting into simulations, for instance, the wire feeding speed. As shown in Fig. 3 the part of the power density is delivered to the base material by Goldak Gaussian distribution, while another part of power density is delivered to filler material with a volume of a cylinder or a rectangle block. This allows to obtain the steep temperature gradients in the molten pool, accurately positioning two heat sources on the top of filler material and the base material respectively. In reality the correct amount of heat to the filler material elements is transmitted.

The power density function is presented in Eq. (6)

$$
\begin{cases}
\dot{q}_b = \dfrac{6\sqrt{3}f_f \dot{Q}_{bf,r}}{a_{f,r}bc\pi\sqrt{\pi}} \exp\left(-\dfrac{3[x+v(\tau-t)]^2}{a_{f,r}^2} - \dfrac{3y^2}{b^2} - \dfrac{3z^2}{c^2}\right) \\
\dot{q}_w = \dfrac{\dot{Q}_w}{Vel}
\end{cases}
\tag{6}
$$

where Q_b and Q_w are the total powers transmitted respectively to the base and filler material. According to literature, the amount of total power consumed in melting filler material is roughly 50% [18], Hence Q_b and Q_w can be written as:

$$
\dot{Q}_w = \dot{Q}_b = \frac{nIV}{2}
\tag{7}
$$

In Fig. 3 the cylinder bloke represents the volume of wire filler elements to be melted. The power density value $\dot{q}_w$ is defined as the ratio of the wire melting power to the volume of the elements currently heated by the heat source, as shown in Eq. (8). The volume depends on the heat source size along feed direction, where l is feeding length. To transmit the correct amount of energy to filler FE elements the value of such parameter must be defined, i.e.

$$
\dot{q}_w = \frac{\dot{Q}_w}{v} = \frac{\dot{Q}_w}{v_f w_L h_i}
\tag{8}
$$

where v_f represents the moving speed of the arc torch. This value should be equal to the energy per unit volume actually transmitted to the workpiece in the FE model. In practical thermal FE analysis the energy per unit volume transmitted to filler can be computed as

$$\dot{q}_w = \frac{\dot{Q}_w}{v_{e_l}}\tau = \frac{\dot{Q}_w}{w_l h_l d_{e_l}} \frac{l}{v_f} \tag{9}$$

where v_{el} is the volume of molten filler elements, τ is the time interval from the centroids of the FE elements corresponding to a single segment to the next centroids. Therefore, the torch head moving speed and filler feeding velocity are related to heat power density rate. The heat source dimension in feed direction must be equal to the correspondent size of filler FE elements [17].

2.2 Validation of Heat Source Model

Both Goldak double ellipsoid and modified Goldak heat source models are implemented in Abaqus CAE 2019 user subroutine DFLUX. Comparison of the simulation results are presented in Fig. 4.

An additive manufacturing plate model for validation of heat source is created in Abaqus CAE 2019, using Python script to form sets and steps for thermal analysis. Element activation and interaction algorithm (model change) are used for material deposition. The detail parameters and steps will be discussed in section of validation of the experiment. Figure 4a shows the temperature distribution computed using modified Goldak model. Figure 4b is the result by using Goldak double ellipsoid
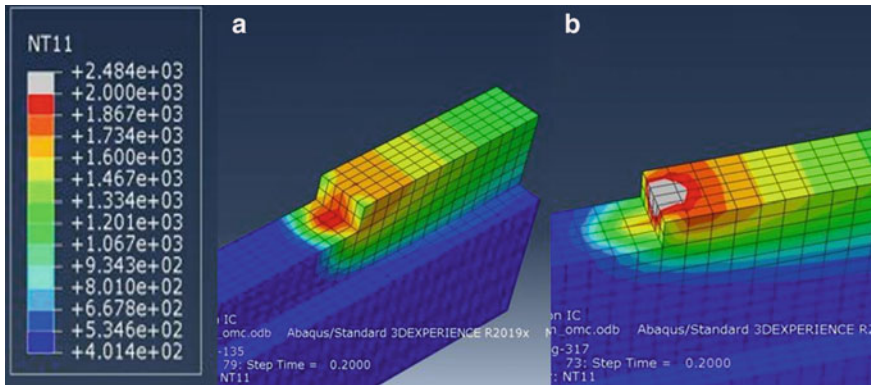

Fig. 4 Temperature distributions: **a** modified model **b** Goldak model

Table 1 Parameters for heat source model [mm]

a_f	a_r	b	C	f_f	f_r	ι
1.8	5.0	3.0	5.0	1.0	1.0	1.8

heat source model. Table 1 lists the 3D parameters for heat source model valida-
tion corresponding to Figs. 2 and 3. The heat power density Eqs. (6) and (9) were
implemented in Abaqus using user routine DFLUX with all key parameters.

The test plate is 6 mm in the width, base material is low carbon alloy steel S700.
The melting temperature.

From simulation results the temperature distribution of molten pool are apparently
different. Goldak model Fig. 4b has higher temperature in the upper region (grey
color) than the one of modified model Fig. 4a. As discussed in the previous Sect. 2.2
the modified Goldak model distribute heat power to filler and base. In the simulation
two troch heads are positioned on the top of the filler and above the base actually
in the filler elements. Therefore overheat zone appears on the result by Goldak
model (Fig. 4b) Correct temperature distribution is very important for the calculations
of thermal stress, deformation, cracks, and microstructure as well as mechanical
properties of the component printed by WAAM.

3 Validation of the Heat Transfer Model

3.1 Experimental Test

An experimental test plate made by WAAM processing is simulated. Using Abaqus
CAE and the user subroutines, Python scripts thermal-metalogic-mechanical models
are fully implemented. Validations of thermal analyses are presented as follows [19].

1. The configuration used in tests:

   - Substrate: 15 mm thickness mild carbon steel
   - Wire material: G4Si1/AWS 5.18 ER70S-6 Ø1.0 mm Böhler Union K56
   - Shielding gas: Air Liquide Arcal Force (92/8% Ar-CO_2) flow rate 20 l/min

2. See Table 2.
3. Printing strategy
   Printing of each layer, waiting with an incremental time (+2 s every layer) before
   and after forced cooling. Figure 5 is the procedure of the printing. The interval
   cooling time each layer is about two minutes.
   The inter-layer temperature was measured by pointing the thermal cursors
   (always in the same pass) just before the passage of the weld pool. The
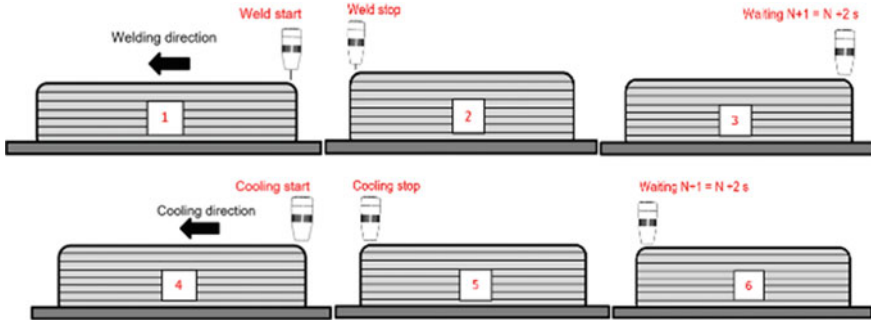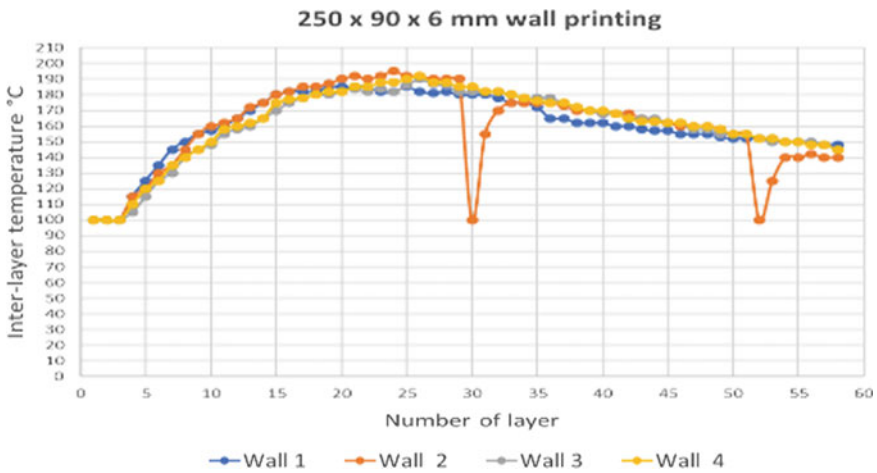   temperature-time curves measured are shown in Fig. 6.
4. The printed test wall

Fig. 5 The procedure of printing process

Wall	Arc time (min)	Cooling time (min)	Total time (min)
1	24.5	131	155.5
2	24.5	146	170.5
3	24.5	131	155.5
4	24.5	131	155.5

Fig. 6 Inter layer temperature curves measured in the printing process

Figure 7 shows a test wall printed by wire arc additive manufacturing process with strategy presented above Table 2 [20].
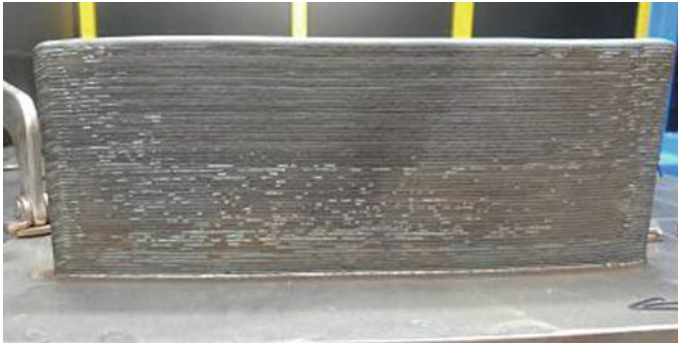
Fig. 7 The test wall printed with parameters above

Table 2 Printing parameters for multi layer walls 120 × 25 × 6 mm

	Root	Start	Middle	End
Job number	1	2	3	4
Length (mm)	120	5	110	5
WFS (m/min)	6.0	5.0	6.0	7.0
U (V)	16.5	15.4	16.5	16.8
I (A)	148	127	148	156
CTWD (mm)	15	15	15	15
TS (cm/min)	60	72	60	48
AL Correction	0	+5	0	-5
DYN Correction	0	0	0	+5
Change Job Ramp (s)	0	0.2	0.2	0.1
Correction S	0	5.0	0	0
t-S	0.2	0.2	0.1	0.2
I-S	50	20	50	20
SL1	0.2	0.1	0.1	0.1
SL2	0.2	0.1	0.1	0.3
t-E	0.2	0.5	0.1	0.5
I-E	30	60	50	25
Correction E	0	0	0	-5

Table 2 (continued)

Acronym	Parameters	Range
CTWD	Contact tip to work distance (mm)	5; 20
WFS	Wire Feed Speed (m/min)	0; 20
TS	Robot Travel Speed (cm/min)	0; 100
S	Correction arc length for arc ignition	-10; 10
t-S	Duration of arc ignition (s)	0; 10
I-S	Percentage of current used for arc ignition (%)	0; 200
SL1	Duration of the ramp between arc ignition and welding state (s)	0; 10
SL2	Duration of the ramp between welding state and arc extinction(s)	0; 10
I-E	Percentage of current used for arc extinction (%)	0; 200
t-E	Duration of arc extinction (s)	0; 10
E	Correction arc length for arc extinction	-10; 10
AL Correction	Correction arc length during welding	-10; 10
DYN Correction	Correction of arc dynamic	-10; 10

3.2 Thermal Simulation Modeling

By using Abaqus CAE 2019 this teat wall ($250 \times 90 \times 6$ mm) is built as a model for simulation. Heat transfer analysis for WAAM process in Abaqus CAE (no plug in modulus) requires some different aspects as follows:

1. Build the part model and choose regional meshing in order to control element numbering and order. This manner will assist to make sets of elements and steps through Python scripts as shown in Fig. 8. Historically adding material is performed by using activation and deactivation of sets of elements. However the
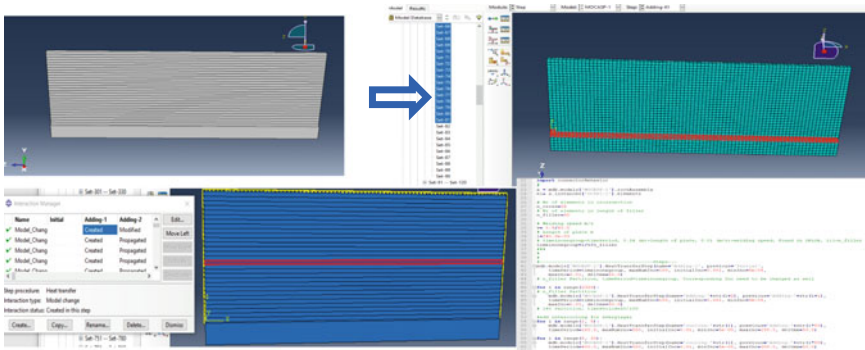

Fig. 8 Main steps required for WAAM simulation

traditional algorithm is not so efficient and the new technique has been in the development in Aabaqus CAE Additive plug in modeler [21].

2. Heat source moving and heat up under layer is achieved by user subroutine DFLUX. As mentioned in the previous sections a modified Goldak ellipsoid model was implemented in FORTRAN code. There are some limitations for WAAM processing, especially for interval parameter variations, multiple torch head moving with different materials, and interval layer forced cooling and so on.

3. Using three algorithms in Abaqus CAE to simulate interval cooling which are film condition, natural convection, cooling flux by DFLUX subroutine.

3.3 Results and Discussion

Heat transfer analyses on the test wall were performed with main parameters in the experiments. Validation is performed by comparing the interval layer temperature measurements of experiments to the results of simulations. Three different approaches for interval cooling have been used in Abaqus/CAE2019. The data of FE models are as follows.

- total number of nodes (type: DC3D8): 9477.
- total number of elements: 6240
- sets of elements for adding materials: 2359, each set includes 2 elements.
- time steps: 2400
- interactions with model change to activate set of elements.

Using natural convection and cooling time for interlayer cooling.

Results of heat transfer simulation during WAAM process are shown in Fig. 9. Four contour plots of temperature distribution when printing, respectively, are shown: (a) layer.5, (b) layer 7, (c) layer 23 and (d) layer 27. Wall temperature increased layer by layer (about 150 °C) when cooling time set as 120 s and internal natural convection
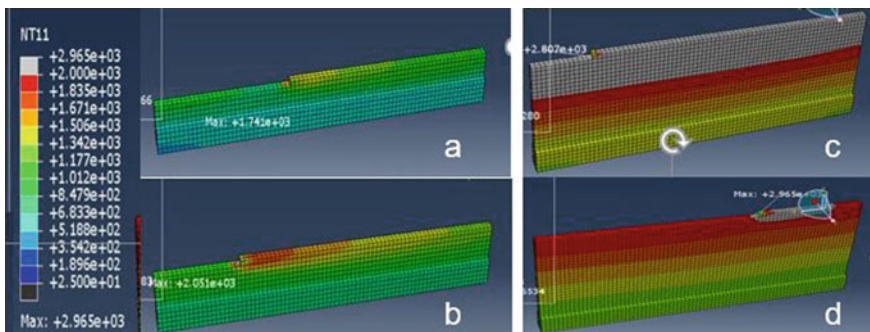

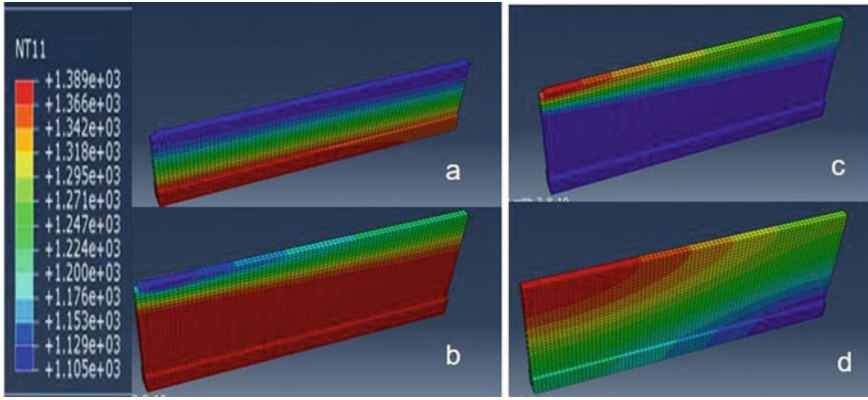**Fig. 9** Temperature distribution during the printing process

Fig. 10 Forced cooling (**a**), **b** chilling layer, **c** adding layer, **d** final cooling

for cooling. The wall temperature is over molten at layer 17 as well, which means wall printing collapse practically. Therefore interval layer cooling is one of crucial and effective parameters for WAAM process.

Due to lack of parameters for forced cooling we tried to use subroutine DFLUX to set up chilling flux and the jet head movement. For quickly testing, the approach of element activation and material properties were kept. The flux for chilling is just given a negative constant value q_c. Figure 10 presents the results of interval forced cooling. Figure 10a and c show that temperature drops down rapidly under the jet flux. If Abaqus AM plug in with user subroutine is able to simulate multi-torch movement and different material properties the approach will be very useful for variant WAAM process.

Eventually surface film condition in Abaqus interactions modeler was used for interval forced cooling (Fig. 11). By adjusting embedded film coefficient f_c, sink temperature and cooling time the temperature curves measured in the experiment could be fitted to although the real jet head movement could not be simulated.

Table 3 summarized main parameters in heat transfer analyses. In Fig. 12 the temperature curve L3 has general agreement with the experimental data in Fig. 6.
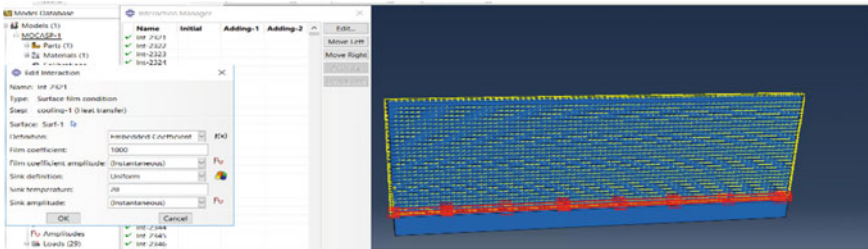

Fig. 11 Surface film condition settings for interval cooling

Table 3 Parameters in the analysis

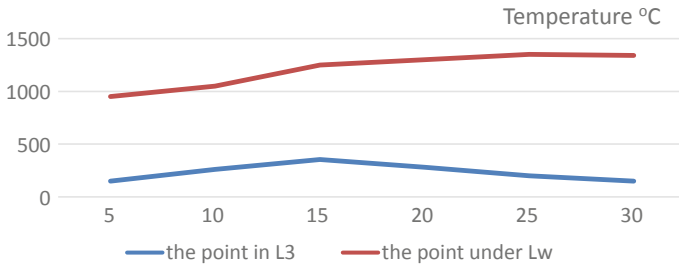| U (v)	I (A)	V_L (cm/min)	V_f (m/min)	L (mm)	t_{inc} (S)	f_c
16	150	60	6.0	240	120	100

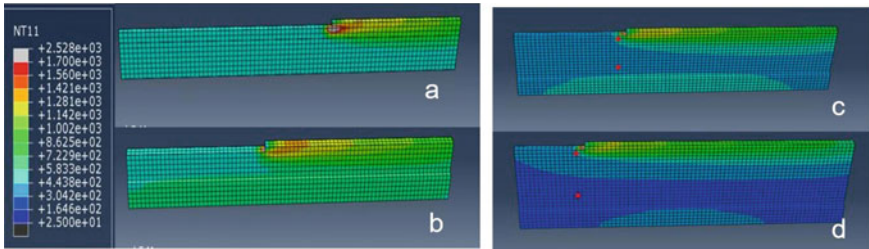**Fig. 12** Temperature curves measured in simulation

Fig. 13 The temperature distribution in the printing process

The curve L_w is the temperature measured under layer of the current weld pass. Figure 13a–d represent the temperature distribution in the printing process. Therefore thermal FE modelling for WAAM process is successfully implemented via user subroutine. However for simulation on real parts the computation capacity and time consuming are still in challenges.

4 Conclusions

In this work the modified Goldak heat source model is applied to the wire arc additive processing simulation by using Abaqus CAE 2019 and user subroutine. The advantage of modified Goldak model allows to take into account the feeding speed of filler material and resulting in correct energy input for heat transfer FE analyses.

Element activation algorithm is successfully used in WAAM simulation through Abaqus Python scripts and user subroutines. Hopefully the operation and time consuming will be improved by using Abaqus CAE Plugin modrler later.

Key parameters play key roles in the printing process such as heat input energy and interval cooling (or cooling flux and time).

The future work will do further improvement on the efficiency and accuracy for simulation, meanwhile microstructure, properties prediction models and residual stress analysis will be applied to the experimental model plate.

References

1. Ding D, Pan Z, Cuiuri D, Li H (2015) Wire-feed additive manufacturing of metal components: technologies, developments and future interests. Int J Adv Manuf Technol 81:465–481
2. Ding D, Pan Z, Cuiuri D, Li H (2015) A multi-bead overlapping model for robotic wire and arc additive manufacturing (WAAM). Robot Comput Integr Manuf 31:101–110
3. Application Form for SIM ICON Project Version of this document. January (2016)
4. Rodrigues TA, Duarte V et al (2019) Current status and perspectives on wire and arc additive manufacturing (WAAM). Materials 12(7):1121
5. Martina F, Ding J, Williams S, Caballero A, Pardal G, Quintino L (2018) Tandem metal inert gas process for high productivity wire arc additive manufacturing in stainless steel. Addit Manuf 2018(25):545–550. https://doi.org/10.1016/j.addma.11.02
6. Almeida PMS, Williams S (2010) Innovative process model of Ti–6AL–4V additive layer manufacturing using cold metal transfer (CMT). In: Proceedings of the 21st international solid freeform fabrication symposium. Austin, TX, USA, 1–9
7. Xie Y, Zhang H, Zhou F (2016) Improvement in geometrical accuracy and mechanical property for arc-based additive manufacturing using metamorphic rolling mechanism. J Manuf Sci Eng 138:111002. https://doi.org/10.1115/1.4032079
8. ASTM F2792-12a (2012) Standard terminology for additive manufacturing technologies (Withdrawn 2015). ASTM International: West Conshohocken, PA, USA
9. Ni J, Voorde J Vande, Antonissen J, Wahab MA (2018) Dependency of phase transformation on the prior austenite grain size and its influence on welding residual stress of s700 steel. Weld World 1–14
10. Ni J (2019) Improved residual stress prediction of welded steel components. Ph.D. thesis, Soete Laboratory, Ghent University
11. Pavelic V (1969) Experimental and computed temperature histories in gas tungsten arc welding of thin plates. Weld J Res Suppl 48:296–305
12. Krutz WG, Segerlind JL Finite element analysis of welded structures. Weld Res Suppl 211–216
13. Goldak JA, Akhlaghi M (2016) Computational welding mechanics. Springer Science & Business Media
14. Chakravarti GJA, Bibby M (1984) A new finite element model for welding heat sources. Metall Trans B 15(2):299–305
15. Hao M, Sun Y (2013) A FEM model for simulating temperature field in coaxial laser cladding of TI6AL4V alloy using an inverse modeling approach. Int J Heat Mass Transf 64:352–360
16. Goldak J, Chakravarti A, Bibby M (1984) A new finite element model for welding heat sources. Metall Trans B 15:299–305
17. Montevecchi F, Venturini G, Scippa A, Campatelli G (2016) Finite element modelling of wire-arc-additive-manufacturing process. Procedia CIRP 2016(55):109–114. https://doi.org/10.1016/j.procir08.024

18. Dupont JN, Marder AR (1995) Thermal efficiency of arc welding processes. Weld Res Suppl 406–416
19. Goldak J, Bibby M, Moore J, House R, Patel B (1986) Computer modeling of heat flow in welds. Metal Trans B 17:587–600
20. Antonissen J, Vande Voorde J et al (2020) Internal Experimental test report
21. Abaqus (2017) Introduction to user subroutines for AM